RSC Advances

ROYAL SOCIETY OF CHEMISTRY

www.rsc.org/advances

In situ chemical oxidative graft polymerization of aniline from phenylamine end-caped poly(ethylene glycol)-functionalized multi-walled carbon nanotubes

Bakhshali Massoumi[1], Vahideh Badr-Valizad[1], and Mehdi Jaymand[*, 2]

1. Department of Chemistry, Payame Noor University, P.O. BOX: 19395-3697 Tehran, Islamic Republic of Iran.
2. Research Center for Pharmaceutical Nanotechnology, Tabriz University of Medical Sciences, P.O. Box: 51656-65811, Tabriz, Islamic Republic of Iran.

[*] Correspondence to: Mehdi Jaymand, Research Center for Pharmaceutical Nanotechnology, Tabriz University of Medical Sciences, Tabriz, Iran.

Tel: +98-41-33367914; Fax: +98-41-33367929

Postal address: Tabriz-5165665811-Iran

E-mail addresses: m_jaymand@yahoo.com; m.jaymand@gmail.com; jaymandm@tbzmed.ac.ir

Abstract

This paper describes the *in situ* chemical oxidative graft polymerization of aniline from phenylamine end-caped poly(ethylene glycol)-functionalized multi-walled carbon nanotubes (MWCNTs). To aim this purpose, MWCNTs were carboxylated (MWCNTs-COOH) by conventional acid oxidation process, and then poly(ethylene glycol) (PEG) chains were covalently attached to the carboxylated MWCNTs *via* a esterification reaction. The poly(ethylene glycol)-functionalized multi-walled carbon nanotubes (MWCNTs-PEG) was further reacted with *p*-antranilic acid (4-aminobenzoic acid) to produce phenylamine end-caped poly(ethylene glycol)-functionalized multi-walled carbon nanotubes (MWCNTs-PEG-NH_2). The graft polymerization of aniline monomers onto MWCNTs-PEG-NH_2 was initiated by oxidized phenylamine groups after addition of ammonium peroxydisulfate (APS), and *p*-toluene sulfonic acid (*p*-TSA)-doped polyaniline was grown onto functionalized multi-walled carbon nanotubes *via* an oxidation polymerization method. The chemical structures of all samples as representatives were characterized by means of Fourier transform infrared (FTIR) spectroscopy. Moreover, electrical conductivity, electroactivity, optical properties, thermal behaviors, and morphologies of the synthesized samples were studied.

1. Introduction

It is a decisive fact that intrinsically conductive polymers (ICPs) have attracted more and more attention on the basis of their importance in basic scientific research and promising industrial applications, due to their unique physicochemical properties [1-3]. Among the large family of the conductive polymers, polyaniline (PANI), polypyrrole (PPy), and polythiophene (PTh) are important members, and could be incorporated in various practical and technological applications due to their stabilities, and unique physicochemical properties [4-6]. In addition, these conducting polymers have generated a great deal of interest due to their low-cost synthesis (*via* electrochemical or chemical oxidation polymerization), chemical and electronic properties, unique redox tunability, environmental and thermal stability, wide range of commercial and technological applications, and many more [7, 8]. In this respect polyaniline (PANI) and its derivatives have stimulated great interest in the development of organic materials for optical, electronic, and biomedical applications. Polyaniline could be incorporated in various applications such as secondary batteries [9], electromagnetic interference (EMI) shielding [10], solar cells [11], bio/chemical sensors [12], biomedical sciences (*e.g.* tissue engineering performance) [13], corrosion devices [14], electrochromic devices [15], organic light emitting diodes (OLEDs) [16], and many more.

Since the discovery of the carbon nanotubes (CNTs) by Iijima in 1991 [17], due to its exceptional electrical, and mechanical properties combined with chemical stability, it has been become a potential prospective candidate for a wide range of practical and technological applications such as chemical sensors, gas storage, field emission materials, catalyst support, electronic devices, advanced nanocomposites, biomedical sciences, *etc*. [18-20].

However, some drawbacks of carbon nanotubes such as the low processability, and strong interaction between individual CNTs restrict its application range in different fields. Thus modification of CNTs is an immensely important in modern material science for expanding them application fields, and has been the subject of investigation [21, 22]. In the field of polymer/CNTs nanocomposites the good dispersion and good interfacial adhesion between CNTs, and the polymer matrix is necessary to enhance the physicochemical properties of nanocomposites [23, 24]. In order to surface modification of CNTs, well established techniques are: covalent and non-covalent functionalization of CNTs [25, 26]. Covalent functionalization of CNTs has been extensively studied, and many successful approaches have been developed. Generally, long alkyl chains, polymer chains, and biomolecules can be attached onto CNTs by various chemical reactions [27-30]. However, carboxylation is the main commonly known approach in order to produce stable water dispersion of carbon nanotubes, and for further CNTs functionalization *via* carboxylic groups [31, 32].

On the other hand, it is well established that one plausible strategy to upgrade the electrical performances of the conductive polymers is incorporation of carbon nanotubes in the polymer matrix. These (nano-)composite materials showing great potential applications such as supercapacitors, actuators and electronic devices [18, 23]. In ICPs/CNTs (nano-)hybrids a layer of conducting polymer is strongly attached to the carbon nanotube surface through the π-π interactions between the polymer chains and the carbon nanotubes. The polymer layer both prevents nanotube bundling and significantly modifies the mechanical and electronic properties of the (nano-)hybrid structure [33, 34].

In this work, we present the *in situ* chemical oxidative graft polymerization of aniline from phenylamine end-caped poly(ethylene glycol)-functionalized multi-walled

carbon nanotubes (MWCNTs-PEG-NH_2). The electrical conductivity, electroactivity, optical properties, thermal behavior, and morphology of the synthesized MWCNTs-PEG-PANI nanocomposite were studied.

2. Experimental

2.1. Materials

Multi-walled carbon nanotubes (95% purity) with an average diameter and length of about 40–70 nm and 20 μm, respectively, were provided from Research Institute of Petroleum Industry (Tehran, Iran). The thermal and chemical purifications of the MWCNTs and synthesis of carboxylated multi-walled carbon nanotubes (MWCNTs-COOH) were carryout as described in our previous work [18]. Poly(ethylene glycol) (average molecular weight: 2000 g mol^{-1}) was purchased from Merck (Darmstadt, Germany). Aniline monomer (Merck) was distilled under a reduced pressure before use. Dimethylaminopyridine (DMAP), *N*,*N*-dicyclohexyl carbodiimide (DCC), *p*-toluene sulfonic acid (*p*-TSA), *p*-antranilic acid, nitric acid (65%), and sulfuric acid (95–97 %), were provided from Merck, and were used as received. Ammonium peroxydisulfate (APS) from Merck was re-crystallized at room temperature from ethanol–water. Xylene (Merck) was dried by refluxing over sodium and distilled under argon before use. All other reagents were purchased from Merck and purified according to the standard methods.

2.2. Synthesis of poly(ethylene glycol)-functionalized multi-walled carbon nanotubes (MWCNTs-PEG)

In a 100 ml three-neck round-bottom flask equipped with a condenser, gas inlet/outlet, and a magnetic stirrer, 0.2 g (0.97 mmol) *N*,*N*-dicyclohexyl carbodiimide (DCC), and 0.02 g (0.16 mmol) dimethylaminopyridine (DMAP) were dissolved in 20 ml *N*,*N*-dimethylformamide (DMF). In a separate container, 0.3 g of MWCNTs-COOH was

suspended in 20 ml of dried DMF under ultrasonic treatment for 20 minutes. This suspension was de-aerated by bubbling highly pure argon for 20 minutes, and added to the above flask. The reaction mixture was stirred vigorously at room temperature for about 1 hour under argon atmosphere, and then 4 g of the poly(ethylene glycol) was added to the flaks. The reaction mixture was stirred at room temperature for about 48 hours under argon atmosphere. The crude product was vacuum filtered through a poly(tetrafluoroethylene) membrane, and washed with DMF, and distilled water for several times, and dried in vacuum at room temperature.

2.3. Synthesis of phenylamine end-caped poly(ethylene glycol)-functionalized multi-walled carbon nanotubes (MWCNTs-PEG-NH_2)

A 100 ml three-neck round-bottom flask equipped with a dean-stark trap, gas inlet/outlet, and a magnetic stirrer, were charged with anhydrous xylene (50 ml), MWCNTs-PEG (0.3 g), *p*-antranilic acid (0.2 g, 2.8 mmol), and a catalytic amount of *p*-TSA (0.05 g, 0.27 mmol). The reaction mixture was de-aerated by bubbling highly pure argon for 10 minutes, and then the reaction mixture was heated up to 150 °C for about 5 hours. The water of the reaction was removed as an azeotrope until no more water was formed. It could mean that the reaction had gone to completion. At the end of this period, the reaction flask was rapidly cooled to room temperature by ice-water bath. The crude product was vacuum filtered through a poly(tetrafluoroethylene) membrane, and washed with DMF for several times, and dried in vacuum at room temperature.

2.4. Grafting of aniline onto MWCNTs-PEG-NH_2

A 100 ml two-neck round-bottom flask equipped with a condenser, dropping funnel, and a magnetic stirrer, were charged with distilled water (20 ml), aniline (1 g, 10.7 mmol), and *p*-toluene sulfonic acid (4.5 g, 23.2 mmol). In a separate container, 0.2 g

of MWCNTs-PEG-NH_2 was suspended in 10 ml of dried DMF under ultrasonic treatment for 20 minutes. This suspension was added to the above flask, and the reaction mixture was stirred vigorously for about 1 hour. At the end of this period, temperature was reduced to 0 °C, and then 20 ml of oxidant (APS) solution (0.5 mol l^{-1}) was slowly added at a rate of 5 ml min^{-1} to the reaction mixture. The mixture was stirred for about 24 hours at 0 °C. The crude product was filtered, washed several times with methanol, and dried in vacuum at room temperature. To remove the un-grafted PANI chains from the crude product, the powder was extracted with *N*-methylpyrrolidone (NMP) in a Soxhlet apparatus for 24 hours. The obtained black powder, washed several times with NMP, and dried under vacuum at room temperature.

2.5. Synthesis of homo polyaniline (PANI)

In a typical experiment, the pure PANI was synthesized *via* a chemical oxidation polymerization method as follows. A 100 ml two-neck round-bottom flask equipped with a condenser, dropping funnel, and a magnetic stirrer, were charged with distilled water (20 ml), DMF (10 ml), aniline (1 g, 10.7 mmol), and *p*-toluene sulfonic acid (4.5 g, 23.2 mmol). The reaction mixture was vigorously stirred, and temperature was reduced to 0 °C. In a separate container, (2.28 g, 10 mmol) of oxidant (APS) was dissolved in distilled water (20 ml). The oxidant solution was slowly added at a rate of 5 ml min^{-1} to the reaction mixture. The mixture was stirred for about 24 hours at 0 °C. The crude product was filtered, washed several times with methanol, and dried in vacuum at room temperature.

2.6. Electrochemical system

The electrochemical measurements were carried out using Auto-Lab equipment (ECO Chemie, Utrecht, The Netherlands) equipped with a three-electrode cell assembly.

The system was run on a PC using NOVA 1.8 and FRA software. A glassy carbon microelectrode (with a surface area of 0.03 cm^2), a platinum rod, and Ag/AgCl (3 M in KCl) were used as working, counter, and reference electrodes, respectively (all electrodes from metrohm). All potentials applied between working and counter electrode, so the final current measured between working and reference electrode. The surface of the working electrode was polished with emery paper followed by 0.5 μm alumina, and then washed with acetone. The working electrode coated with the synthesized sample was prepared by casting. For this purpose, the samples were dissolved in tetrahydrofuran (THF) to form a 1.0 mg ml^{-1} solution and ultrasonically treated for 15 minutes. The solution was dropped onto the GC microelectrode surface and allowed to dry under ambient conditions. The electrochemical measurements were accomplished in the *p*-toluene sulfonic acid (0.75 mol l^{-1}) by applying a sequential linear potential scan rate of 25–225 mVs^{-1} between -0.4 and 0.9 V *versus* the Ag/AgCl electrode. All experimental solutions were de-aerated by bubbling highly pure argon for 10 minutes, and an argon atmosphere was kept over the solutions during the measurements.

2.7. Characterization

Fourier transform infrared (FTIR) spectra of the samples were recorded on a Shimadzu 8101M FTIR (Shimadzu, Kyoto, Japan). The samples were prepared by grinding the dry powders with potassium bromide (KBr), and compressing the mixture into disks. The spectra were recorded at room temperature. Thermal properties of the samples were examined by thermogravimetric analyzer (TGA-PL STA 1640 equipment (Polymer Laboratories, Shropshire, UK)). The TGA experiments were conducted under nitrogen atmosphere in a temperature range of 25–750 °C with heating rate of 10 °C min^{-1}. The field emission scanning electron

microscope (FE-SEM) type 1430 VP (LEO Electron Microscopy Ltd, Cambridge, UK) was applied to determine the morphologies of the synthesized samples. Transmission electron microscopy (TEM) was performed on a Philips CM10-TH microscope (Phillips, Eindhoven, The Netherlands) with a 100 kV accelerating voltage. UV–visible absorption spectra of the samples were measured using a Shimadzu 1601PC UV-vis spectrophotometer (Shimadzu, Kyoto, Japan) in the wavelength range 300–1000 nm. Electrochemical experiments were conducted using Auto-Lab PGSTA T302N. The electrochemical cell contained five openings: three of them were used for the electrodes and two for argon bubbling in the solutions during all experiments. The four-probe technique (Azar Electrode, Urmia, Iran) was used to measure the conductivity of the synthesized samples at room temperature.

3. Results and discussion

In last decades, there has been growing interest in the development of (nano-)hybrid materials in order to obtain materials with synergetic or complementary behavior for various practical and technological applications. In this respect, intrinsically conductive polymers/carbon nanotubes (ICPs/CNTs) nanocomposites have stimulated great interest, in part due to their enhanced physicochemical properties such as electrical conductivity in comparison with pure conductive polymer. This article consists of four parts: (1) synthesis of carboxylated, and poly(ethylene glycol)-functionalized multi-walled carbon nanotubes, (2) synthesis of phenylamine end-caped poly(ethylene glycol)-functionalized multi-walled carbon nanotubes (MWCNTs-PEG-NH_2), (3) *in situ* chemical oxidative graft polymerization of aniline from MWCNTs-PEG-NH_2, and (4) synthesis of pure polyaniline. The methodologies are shown in Schemes 1 and 2.

(Schemes 1)

(Schemes 2)

3.1. Synthesis of MWCNTs-PEG-NH_2

To produce active sites onto poly(ethylene glycol)-functionalized MWCNTs for grafting of PANI, phenylamine groups were added to the PEG-functionalized MWCNTs. Then, to generate active sites onto MWCNTs, after the PEGylation, *p*-antranilic acid was reacted with MWCNTs-PEG in the presence of *p*-toluene sulfonic acid as the dehydrating agent to produce the MWCNTs-PEG-NH_2. The FTIR spectra of the PEG, MWCNTs-PEG, and MWCNTs-PEG-NH_2 are shown in Figure 1.

The FTIR spectrum of the poly(ethylene glycol) shows the characteristic absorption bands due to the stretching vibrations of aliphatic C–H (2950-2800 cm^{-1}), hydroxyl stretching vibration (3468 cm^{-1}), -CH_2 bending vibrations (1473 and 1356 cm^{-1}), and C-O stretching vibration at 1109 cm^{-1}. The FTIR spectrum of the MWCNTs-PEG shows all the characteristic bands of poly(ethylene glycol), and the weak bands attributable to the MWCNTs. The most distinctive feature in the FTIR spectra of PEG and MWCNTs-PEG is the presence of a new band at 1731 cm^{-1}, corresponding to the stretching vibration absorbance of carbonyl (C=O) groups. After incorporation of phenylamine groups into the MWCNTs-PEG some new bands are observed in the FTIR spectrum of the MWCNTs-PEG-NH_2. The main bands could be listed as aromatic C-H (3083 cm^{-1}), C-N (1027 cm^{-1}), and N-H in the 3250-3200 cm^{-1} region. These FTIR spectra assignments verify that the poly(ethylene glycol)-functionalized multi-walled carbon nanotubes (MWCNTs-PEG), and phenylamine end-caped poly(ethylene glycol)-functionalized multi-walled carbon nanotubes (MWCNTs-PEG-NH_2) were successfully synthesized.

(Figure 1)

3.2. Synthesis of MWCNTs-PEG-PANI

The FTIR spectra of the pure polyaniline (PANI), and MWCNTs-PEG-PANI are shown in Figure 2. The FTIR spectrum of the pure PANI shows the characteristic absorption bands due to stretching vibration of the C=N in the quinoidal units at 1597 cm^{-1}, the benzenoid stretches at 1492 cm^{-1}, $C_{aromatic}$–N stretching at 1308 cm^{-1}, and the N–H stretches at 3286 cm^{-1}. The FTIR spectrum of the MWCNTs-PEG-PANI shows characteristic absorption bands of polyaniline, namely, stretching vibration of the C=N in the quinoidal units at 1597 cm^{-1}, the benzenoid stretches at 1492 cm^{-1}, $C_{aromatic}$–N stretching at 1308 cm^{-1}, and the N–H stretches at 3286 cm^{-1}. In addition, the absorption bands at 2800-2950 (stretching vibration of the aliphatic C–H), 1110 (C-O stretching vibration), and 1709 cm^{-1} (carbonyl stretching vibration) are related to the presence of MWCNTs and PEG in this sample.

(Figure 2)

3.3. Thermal property study

The thermal behaviors of the synthesized samples upon heating under nitrogen atmosphere were investigated by means of thermogravimetric analysis (TGA). The characteristic TGA curves of the MWCNTs (a), MWCNTs-COOH (b), MWCNTs-PEG (c), and pure poly(ethylene glycol) (d) are shown in Figure 3. As seen in this Figure the pristine MWCNTs (Figure 3a), were more stable, and did not show any dramatic decomposition in the temperature range 50–800 °C. The residue at 800 °C for pristine MWCNTs is 96 wt.%. However, thermal decomposition of the MWCNTs-COOH is started from 180 °C, and the weight loss increases rapidly from this temperature to about 300 °C, after which the loss rate slows down. The residue at 800 °C for this sample is 88 wt.%, so the weight content of the carboxylic acid groups in the MWCNTs could be calculated from these results. Thus, the degree of acidic-

functionalization from gradual mass loss of the pristine MWCNTs and MWCNTs-COOH suggest that the MWCNTs has been functionalized around 96 – 88 = 8 wt.%. It is evident that the decomposition of the poly(ethylene glycol) (Figure 3d) was occurring in one step around 290–410 °C, after which the loss rate slows down. The residue at 800 °C for pure PEG is 6 wt.%. The characteristic TGA curve of the MWCNTs-PEG exhibits a two-step weight loss process; the first step corresponds to the decomposition of the carboxylic acid groups (180-310 °C), whereas the second step is associated with the poly(ethylene glycol) scission (320–470 °C), after which the loss rate slows down. The residue at 800 °C for MWCNTs-PEG sample is 58 wt.%, so from gradual mass loss of the MWCNTs-COOH, and MWCNTs-PEG, we can draw the conclusion that the weight content of the PEG in the MWCNTs-PEG sample is 88 – 58 = 30 wt.%. In addition, higher decomposition temperature of the poly(ethylene glycol) chains in the MWCNTs-PEG sample (320–470 °C) in comparison with pure PEG (290–410 °C), indicated that no polymers adsorbed non-covalently onto the surface of the MWCNTs. The increased thermal stability of the poly(ethylene glycol) chains might be attributed to the strong interfacial forces, and formation of hydrogen bonds between functionalized CNTs and the poly(ethylene glycol) matrix.

(Figure 3)

The characteristic TGA curves of the MWCNTs-PEG-PANI (a), and the pure polyaniline (PANI) (b) are shown in Figure 4. It is evident that the decomposition of the pure polyaniline (Figure 4b) was occurring in one step around 380–520 °C, after which the loss rate slows down, and the residue at 800 °C for this sample is 23 wt.%. However, the MWCNTs-PEG-PANI (Figure 4a) undergoes a two-step decomposition; the first step corresponds to the decomposition of the poly(ethylene

glycol) chains (320–470 °C), whereas the second step is associated with PANI chain scission (470–580 °C), after which the loss rate slows down. Moreover, according to Figure 4a, we can conclude that the weight loss of the sample between 180 and 300 °C is accelerated, mainly because of the dehydration reaction of MWCNTs, followed by the early degradation of the carboxylic groups. The residue at 800 °C for this sample is 28 wt.%. In conclusion, higher thermal stability of the MWCNTs-PEG, and MWCNTs-PEG-PANI is originated from the strong interaction of poly(ethylene glycol), and polyaniline chains with MWCNTs, in part due to their surface carboxyl functional groups, π-π interactions between the PANI chains and the carbon nanotubes, and large aspect ratio and surface area.

(Figure 4)

3.4. Morphology study

Direct and clear evidence of the poly(ethylene glycol), and polyaniline chemically bonded to the MWCNTs were demonstrated not only from TGA and FTIR spectroscopy but also from the field emission scanning electron microscopy (FE-SEM), and transmission electron microscopy (TEM) images. The FE-SEM images of the pure MWCNTs (a), MWCNTs-PEG (b), and MWCNTs-PEG-PANI (c), and TEM image of the MWCNTs-PEG-PANI (d) are shown in Figure 5. As seen in the FE-SEM images the pristine MWCNTs consisting of agglomerated carbon nanotubes. The FE-SEM image of the MWCNTs-PEG shows spongy morphology. However, some agglomeration of carbon nanotubes still exists, although the generally excellent separation of MWCNTs is attributed to the attaching of the PEG chains which separates the previously agglomerated carbon nanotubes. The FE-SEM (Figure 5c) and TEM (Figure 5d) images of the MWCNTs-PEG-PANI sample shows that the

MWCNTs were coated by polyaniline chains, and the surface of the carbon nanotubes appears to be grown well with increased thickness (50 to 90 nm).

(Figure 5)

3.5. Electrical conductivity and electroactivity measurements

Unlike to other type of polymers, π-conjugated polymers exhibit conducting and/or semiconducting behaviors and thus serve as potential candidates for technological and biomedical applications. Moreover, it is to be noted that the conductivity of the polyaniline could be enhanced by the conducting bridge between the PANI domains and carbon nanotubes, in part due to the large aspect ratio, and surface area of the carbon nanotubes [18, 23].

The electrical conductivity of the samples was measured using samples in which the conductive materials were sandwiched between two Ni electrodes at room temperature. The experimental determination was repeated 5 times for each sample to evaluate the sample accuracy. Using the values of current (I), voltage (V), and thicknesses (d) of the samples, the volume specific resistivity (ρ; Ω cm), and subsequently, the electrical conductivity (σ; S cm^{-1}) were calculated using the following formula.

$$\rho = (V/I)\,(\pi/\ln 2)d$$

$$\sigma = 1/\rho$$

The results obtained are summarized in Table 1. It is important to note that the conductivities were preserved for at least 100 hours post fabrication. As shown in Table 1, the electrical conductivity of the carboxylated carbon nanotubes (MWCNTs-COOH) is about 2.18 S cm^{-1}, much lower than that the pristine MWCNTs (4.34 S cm^{-}

[1]). In addition, the electrical conductivity of the MWCNTs-PEG-PANI is lower than that the pure polyaniline, in part due to the presence of insulating poly(ethylene glycol) chains.

(Table 1)

Cyclic voltammetry (CV) has become a powerful tool in many areas of electroanalytical chemistry. It is widely applied to investigate a variety of redox processes. The effect of the potential scanning rate (V) on the peak currents for the pure polyaniline, and MWCNTs-PEG-PANI modified electrodes were studied in the range of 25–225 mV s^{-1} scan rates, in an aqueous solution of *p*-toluenesulfonic acid (0.75 mol l^{-1}).

The CVs of the pure polyaniline (Figure 6a) shows three typical redox couples with anodic peaks approximately at 0.19, 0.54, and 0.65 V *versus* Ag/AgCl electrode. In the case of MWCNTs-PEG-PANI (Figure 6b) in lower scan rates (25–125 mV s^{-1}) three typical redox couples with anodic peaks approximately at 0.21, 0.38, and 0.58 V *versus* Ag/AgCl electrode are observed. The MWCNTs-PEG-PANI at higher scan rates (150–225 mV s^{-1}) shows two typical redox couples with anodic peaks approximately at 0.28, and 0.46 V *versus* Ag/AgCl electrode. As seen in the CVs of the pure polyaniline, and MWCNTs-PEG-PANI samples, current density corresponding to the cathodic(s), and anodic(s) peaks are gradually increased with increasing scan rate, which indicates the electrochemical oxidation/reduction (doping/de-doping) of the casted samples were chemically reversible.

In addition, it is important to note that platinum rod (counter electrode) especially in acidic media produce dissolved Pt ions in the solution as the reaction progresses. The dissolved Pt ions can be reduced at the cathode, resulting in finely divided Pt particles on the film [35].

To evaluate the electroactivity further, it was determined the relationship between the peak current size *versus* scan rate. The linear relationships between the current and scan rate (25–225 mV s^{-1}) in the pure polyaniline, and MWCNTs-PEG-PANI are shown in Figure 7. This linear relationship is typical of a redox active polymer attached to the electrodes, and also exemplifies the stability of the synthesized samples toward doping/de-doping.

On the bases of the evidence from electrical conductivity, and electroactivity measurements the conclusion could be drawn that the synthesized MWCNTs-PEG-PANI nano-hybrid exhibited lower electrical conductivity, and electroactivity than those of the pure polyaniline, in part due to the presence of insulating poly(ethylene glycol) chains. However, the lower electrical conductivity, and electroactivity levels in this material can be improved at the price of processability, physicochemical properties, and biocompatibility due to the presence of poly(ethylene glycol) segments, and MWCNTs nano-material.

(Figure 6)

(Figure 7)

3.6. UV-vis spectroscopy

The optical properties of the synthesized samples were studied using ultraviolet-visible (UV-vis) spectroscopy. The samples for UV-vis spectroscopy were prepared by dissolving the same amount of the obtained samples in *N*-methylpyrrolidone (NMP) followed by ultrasonic treatment for 15 minutes. As seen in Figure 8 the UV-vis spectrum of the pure polyaniline was characterized by two electronic transitions respectively at about 338 and 637 nm. The first absorption band corresponds to the overlap of the π–π* transition of the benzenoid rings of polyaniline, while the latter one is corresponded to the polaron form PANI. However, the UV-vis spectrum of the

MWCNTs-PEG-PANI also was characterized by two electronic transitions at about 314 and 624 nm, respectively. These shifts to shorter wavelength (blue shift) are ascribed to the significantly decreasing of conjugated units concentration by the poly(ethylene glycol) segments in the case of MWCNTs-PEG-PANI in comparison with pure polyaniline.

(Figure 8)

4. Conclusion

In summary, the *in situ* chemical oxidative graft polymerization of aniline from phenylamine end-caped poly(ethylene glycol)-functionalized multi-walled carbon nanotubes (MWCNTs-PEG-NH_2) has been successfully demonstrated. The chemical structures of all samples as representatives were characterized by FTIR spectroscopy. The TGA analysis, FE-SEM and TEM images provided direct and clear evidence for the chemically grafting of PEG-*b*-PANI onto MWCNTs. The synthesized MWCNTs-PEG-PANI nano-hybrid material showed the polaronic band, at lower wavelength (higher energy) than pure polyaniline in the UV-vis spectra due to the decreasing of conjugated units concentration by the poly(ethylene glycol) segments in the case of MWCNTs-PEG-PANI in comparison with pure polyaniline. The cyclic voltammograms (CVs) of the MWCNTs-PEG-PANI exhibited some qualitative similarities with those of pure polyaniline. The CVs of MWCNTs-PEG-PANI sample indicated that the grafted polyaniline onto MWCNTs-PEG-NH_2 still remained a good redox activity in the resulting nano-hybrid, and the synthesized sample was highly stable. The conductivity, and electroactivity measurements exhibited the MWCNTs-PEG-PANI sample has lower electrical conductivity and electroactivity than those of the pure polyaniline. However, the lower electrical conductivity and electroactivity levels can be improved at the price of processability, physicochemical properties, and

biocompatibility due to the presence of poly(ethylene glycol) segments, and MWCNTs nano-material. As results, we envision that the synthesized MWCNTs-PEG-PANI nano-hybrid could find applications in optoelectronic devices due to its redox, conductivity, and processability properties. In addition, the synthesized nano-hybrid material could find applications in biomedical fields such as fabrication of conductive scaffolds to promote neurite outgrowth and nerve regeneration due to its conductivity, and biocompatibility.

Acknowledgement

We express our gratitude to the Payame Noor University, and Research Center for Pharmaceutical Nanotechnology, Tabriz University of Medical Sciences for supporting this project.

References

[1] Y. Shi, C. Ma, L. Peng and G. Yu, *Adv. Funct. Mater.,* 2015, **25**, 1219-1225.

[2] M. Jaymand, *Prog. Polym. Sci.,* 2013, **38**, 1287–1306.

[3] Y. Yin, C. Liu and S. Fan, *Nano Energy*, 2015, **12**, 486-493.

[4] B. Massoumi, N. Sorkhi-Shams, M. Jaymand and R. Mohammadi, *RSC Adv.,* 2015, **5**, 21197–21205.

[5] S.J. Park, H. Zhao, G. Ai, C. Wang, X. Song, N. Yuca, V.S. Battaglia, W. Yang and G. Liu, *J. Am. Chem. Soc.,* 2015, **137**, 2565-2571.

[6] M. Jaymand, M. Hatmazadeh and Y. Omidi, *Prog. Polym. Sci.,* (DOI: 10.1016/j.progpolymsci.2014.11.004).

[7] H.S. Kolla, S.P. Surwade, X. Zhang, A.G. MacDiarmid and S.K. Manohar, *J. Am. Chem. Soc.,* 2005, **127**, 16770–16771.

[8] J. Xie, X. Han, C. Zong, H. Ji and C. Lu, *Macromolecules,* 2015, **48**, 663-671.

[9] D. Zhang, Y. Yin, C. Liu and S. Fan, *Chem. Commun.,* 2015, **51**, 322-325.

[10] H.R. Tantawy, D.E. Aston, J.R. Smith and J.L. Young, *ACS. Appl. Mater. Interface.,* 2013, **5**, 4648-4658.

[11] A. Shit, S. Chatterjee and A.K. Nandi, *Phys. Chem. Chem. Phy.,* 2014, **16**, 20079-20088.

[12] X. Zhou, S. Lee, Z. Xu and J. Yoon, *Chem. Rev.,* (DOI: 10.1021/cr500567r).

[13] J.C.C. Wu, S. Ray, M. Gizdavic-Nikolaidis, B. Uy, S. Swift, J. Jin and R.P. Cooney, *Synth. Met.,* 2014, **198**, 41-50.

[14] S. Pour-Ali, C. Dehghanian and A. Kosari, *Corros. Sci.,* 2015, **90**, 239-247.

[15] E.M. Erro, A.M. Baruzzi and R.A. Iglesias, *Polymer,* 2014, **55**, 2440-2444.

[16] A. Shahalizad, S. Ahmadi-Kandjani, H. Movla, H. Omidi, B. Massoumi, M.S. Zakerhamidi and A.A. Entezami, *Optic. Mater.,* 2014, **37**, 760–765.

[17] S. Iijima, *Nature,* 1991, **354**, 56-58.

[18] B. Massoumi, M. Jaymand, R. Samadi and A.A. Entezami, *J. Polym. Res.,* 2014, **21**, 442.

[19] A. Saha, C. Jiang and A.A. Marti, *Carbon,* 2014, **79**, 1-18.

[20] D. Ge, L. Yang, A. Honglawan, J. Li and S. Yang, *Chem. Mater.,* 2014, **26**, 1678-1685.

[21] H. Yan and K. Kou, *J. Mater. Sci.,* 2014, **49**, 1222-1228.

[22] T. Zhang, M. Tang, L. Kong, H. Li, T. Zhang, Y. Xue and Y. Pu, *J. Hazard. Mater.,* 2015, **284**, 73–82.

[23] C. Oueiny, S. Berlioz and F.X. Perrin, *Prog. Polym. Sci.,* 2014, **39**, 707-748.

[24] A.V. Poyekar, A.R. Bhattacharyya, A.S. Panwar, G.P. Simon and D.S. Sutar, *ACS Appl.Mater. Interface.,* 2014, **6**, 11054-11067.

[25] M. Li, Y. Wu, F. Zhao, Y. Wei, J. Wang, K. Jiang and S. Fan, *Carbon,* 2014, **69**, 444-451.

[26] N. Mukhopadhyay, A.S. Panwar, G. Kumar, I. Samajdar and A.R. Bhattacharyya, *Phys. Chem. Chem. Phys.,* 2015, **17**, 4293-4310.

[27] M. Yu, Y. Zhang, Y. Zeng, M.S. Balogun, K. Mai, Z. Zhang, X. Lu and Y. Tong, *Adv. Mater.,* 2014, **26**, 4724–4729.

[29] B. Tebikachew, S. Magina, D. Mata, F.J. Oliveira, R.F. Silva and A. Barros-Timmons, *Mater. Chem. Phys.,* 2015, **149**, 378-384.

[30] X. Li, J. Lan, M. Ai, Y. Guo, Q. Cai and X. Yang, *Colloid. Surface B.,* 2014, **123**, 753–761.

[31] J.M. Tour, J.L. Hudson, C.R. Dyke and J.J. Stephenson, *International Patent,* WO05113434, 2005.

[32] S. Morales-Torres, T.L. Silva, L.M. Pastrana-Martínez, A.T. Brandão, J.L. Figueiredo and A.M. Silva, *Phys. Chem. Chem. Phys.,* 2014, **16**, 12237-12250.

[33] X. Tian, Q. wang, X. Chen, W. Yang, Z. Wu, X. Xu, M. Jiang and Z. Zhaou, *Appl. Phys. Lett.,* **105**, 2014, 203109.

[34] T.K. Gupta, B.P. Singh, R.B. Mathur and S.R. Dhakate, *Nanoscale,* 2014, **6**, 842-851.

[35] C. Gu, B.C. Norris, F.R.F. Fan, C.W. Bielawski and A.J. Bard, *ACS Catal.,* 2012, **2**, 746−750.

Schemes, Figures, and Table Captions:

Scheme 1. Synthesis of poly(ethylene glycol)-functionalized MWCNTs, phenylamine end-caped poly(ethylene glycol)-functionalized MWCNTs, and MWCNTs-PEG-PANI.

Scheme 2. Synthesis of pure polyaniline.

Figure 1. Fourier transform infrared spectra of the PEG, MWCNTs-PEG, and MWCNTs-PEG-NH_2.

Figure 2. Fourier transform infrared spectra of the pure polyaniline (PANI), and MWCNTs-PEG-PANI.

Figure 3. Thermogravimetric analysis of the MWCNTs (a), MWCNTs-COOH (b), MWCNTs-PEG (c), and pure poly(ethylene glycol) (d).

Figure 4. Thermogravimetric analysis of the MWCNTs-PEG-PANI (a), and pure polyaniline (b).

Figure 5. The FE-SEM images of the pure MWCNTs (a), MWCNTs-PEG (b), and MWCNTs-PEG-PANI (c), and TEM image of the MWCNTs-PEG-PANI (d).

Table 1. The electrical properties of the synthesized samples.

Figure 6. Cyclic voltammetry (CVs) curves of the pure polyaniline (a), and MWCNTs-PEG-PANI nano-hybrid (b).

Figure 7. Linear relationship between current and scan rate in the pure polyaniline, and MWCNTs-PEG-PANI (the currents are related to the first anodic peaks).

Figure 8. Electronic spectra of the pure PANI, and MWCNTs-PEG-PANI in *N*-methylpyrrolidone (NMP) solution.

Schemes, Figures, and Table:

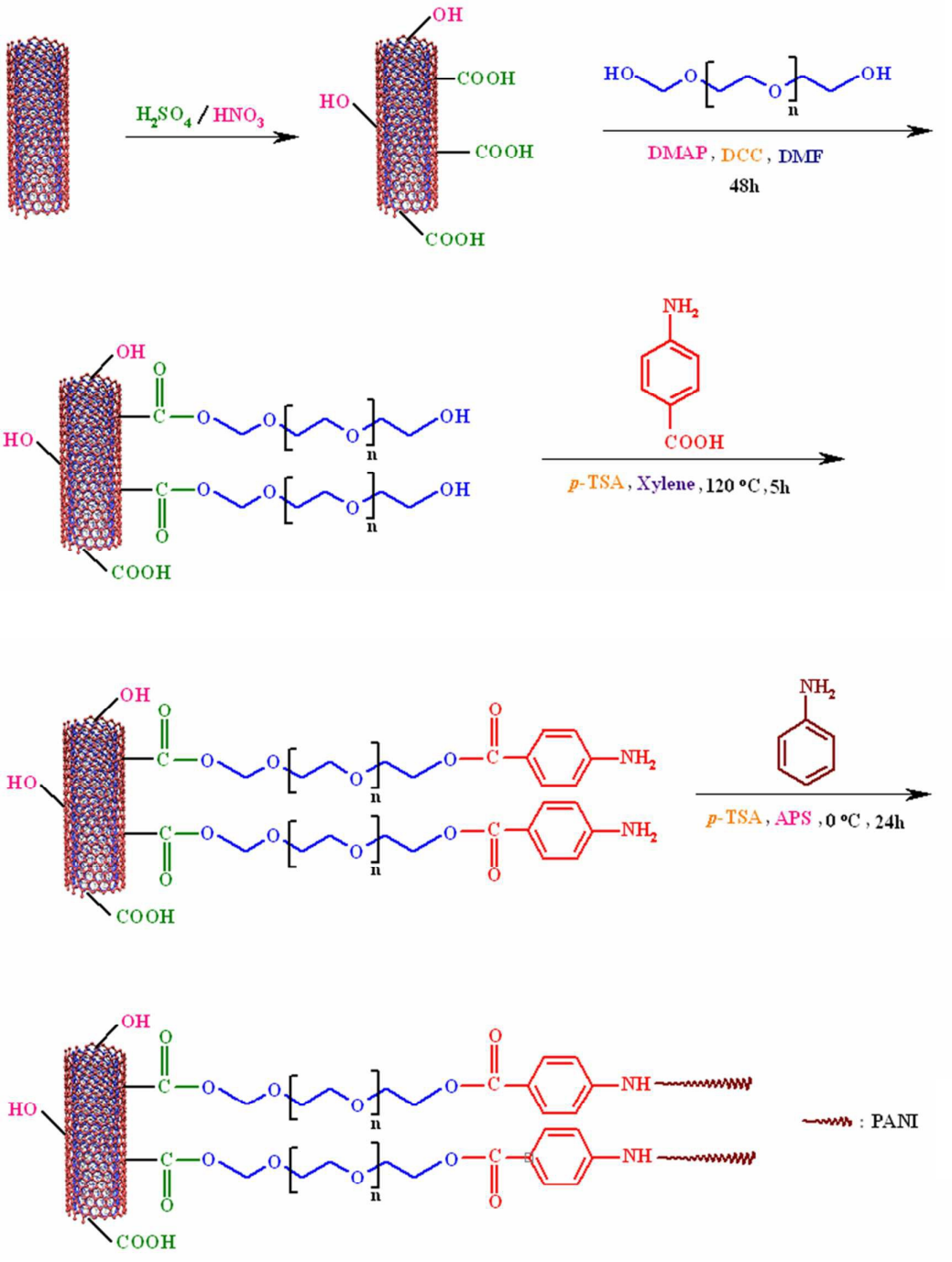

Scheme 1. Synthesis of poly(ethylene glycol)-functionalized MWCNTs, phenylamine end-caped poly(ethylene glycol)-functionalized MWCNTs, and MWCNTs-PEG-PANI.

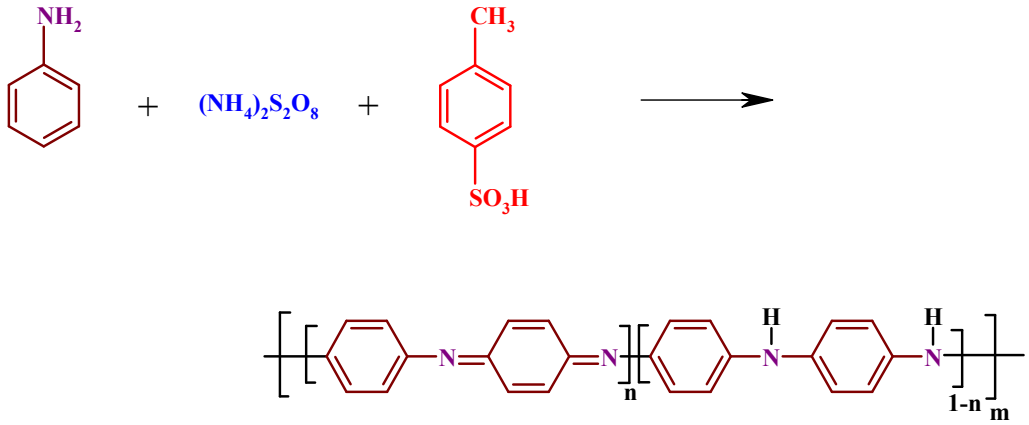

Scheme 2. Synthesis of pure polyaniline.

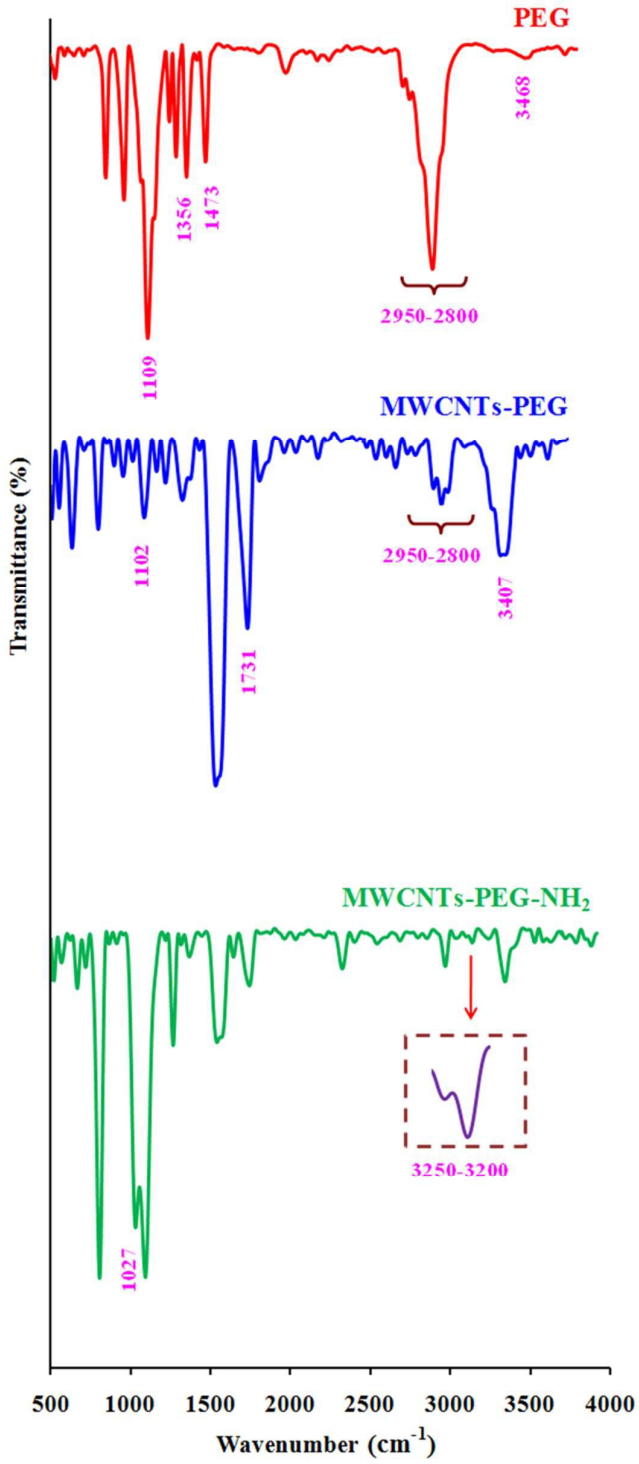

Figure 1. Fourier transform infrared spectra of the PEG, MWCNTs-PEG, and MWCNTs-PEG-NH_2.

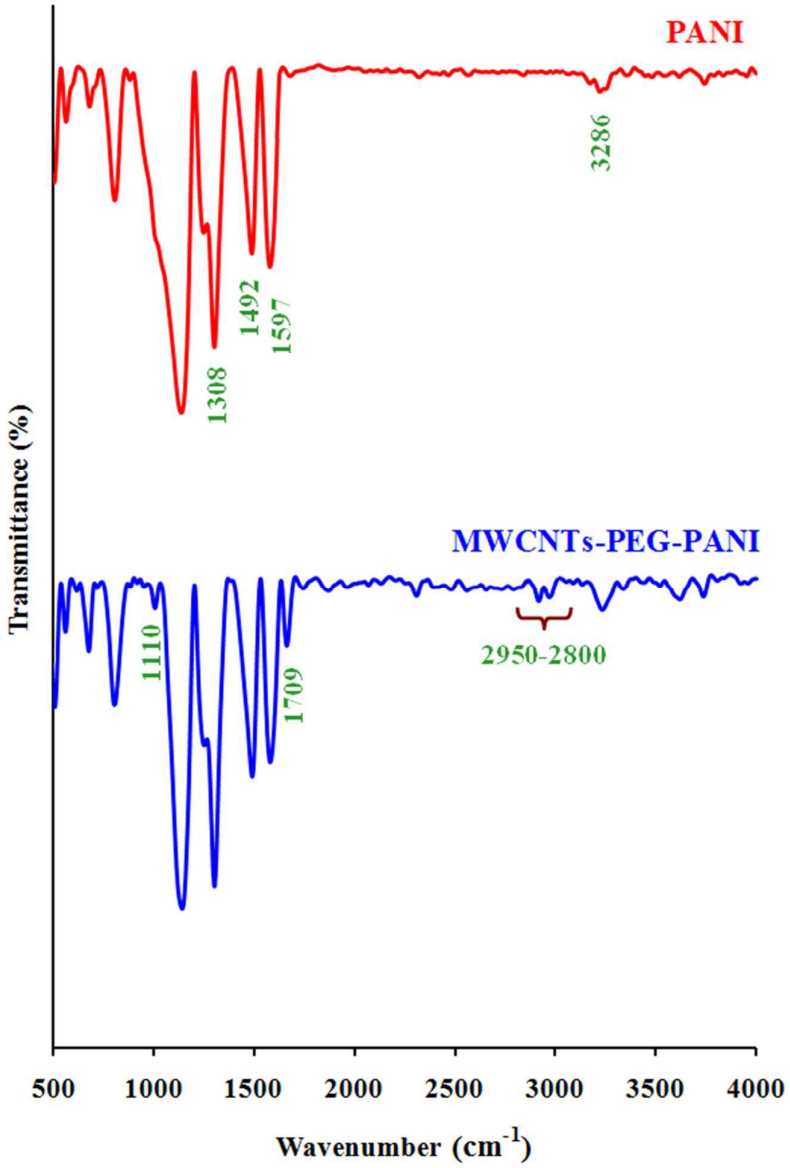

Figure 2. Fourier transform infrared spectra of the pure polyaniline (PANI), and MWCNTs-PEG-PANI.

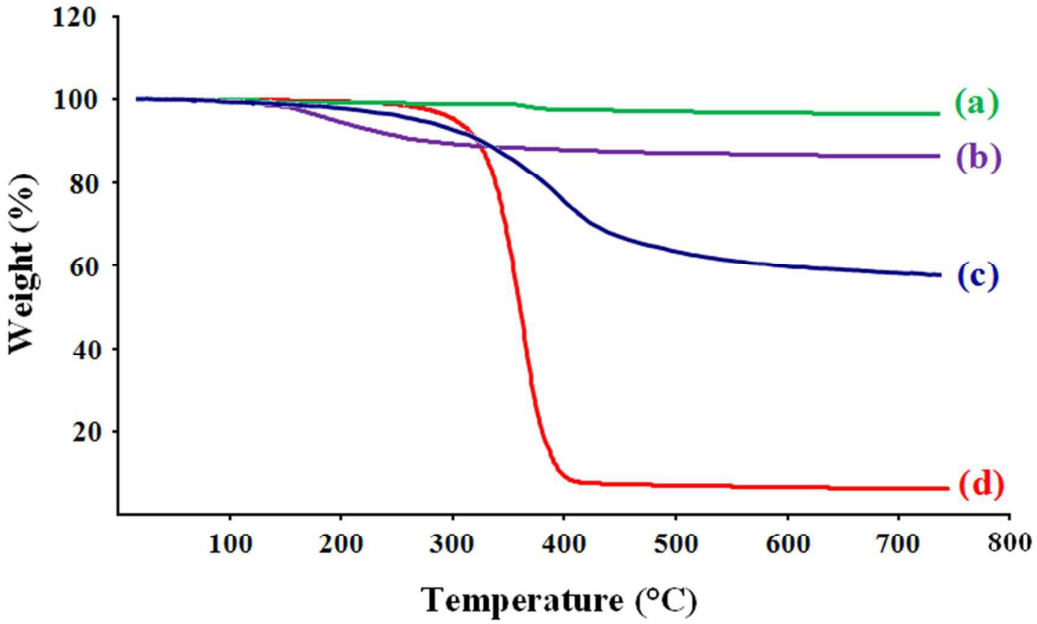

Figure 3. Thermogravimetric analysis of the MWCNTs (a), MWCNTs-COOH (b), MWCNTs-PEG (c), and pure poly(ethylene glycol) (d).

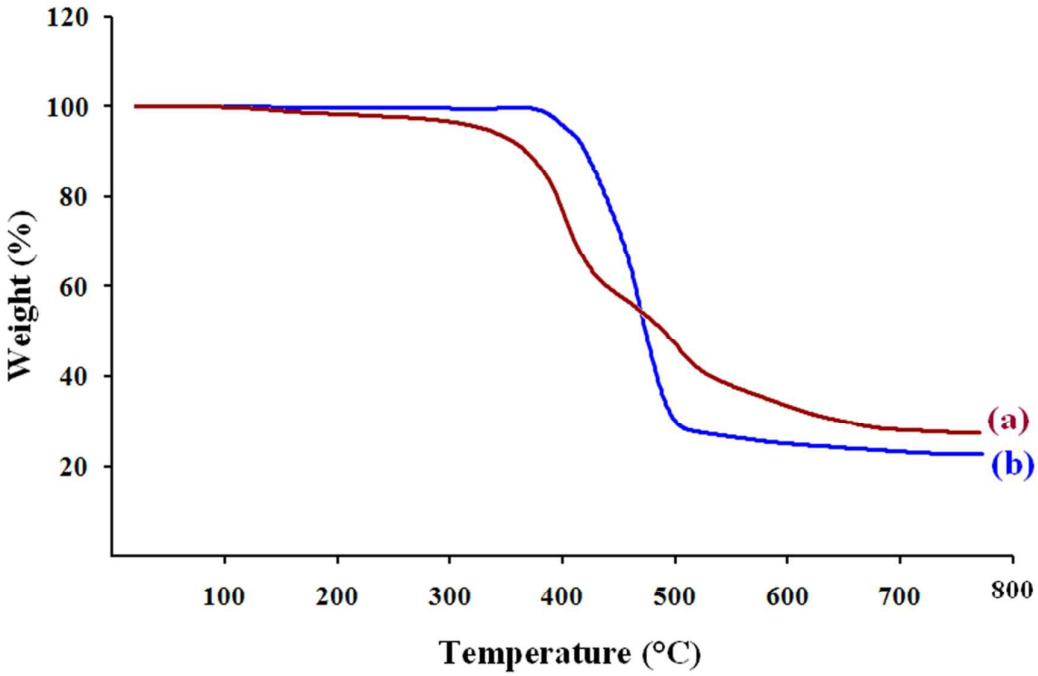

Figure 4. Thermogravimetric analysis of the MWCNTs-PEG-PANI (a), and pure polyaniline (b).

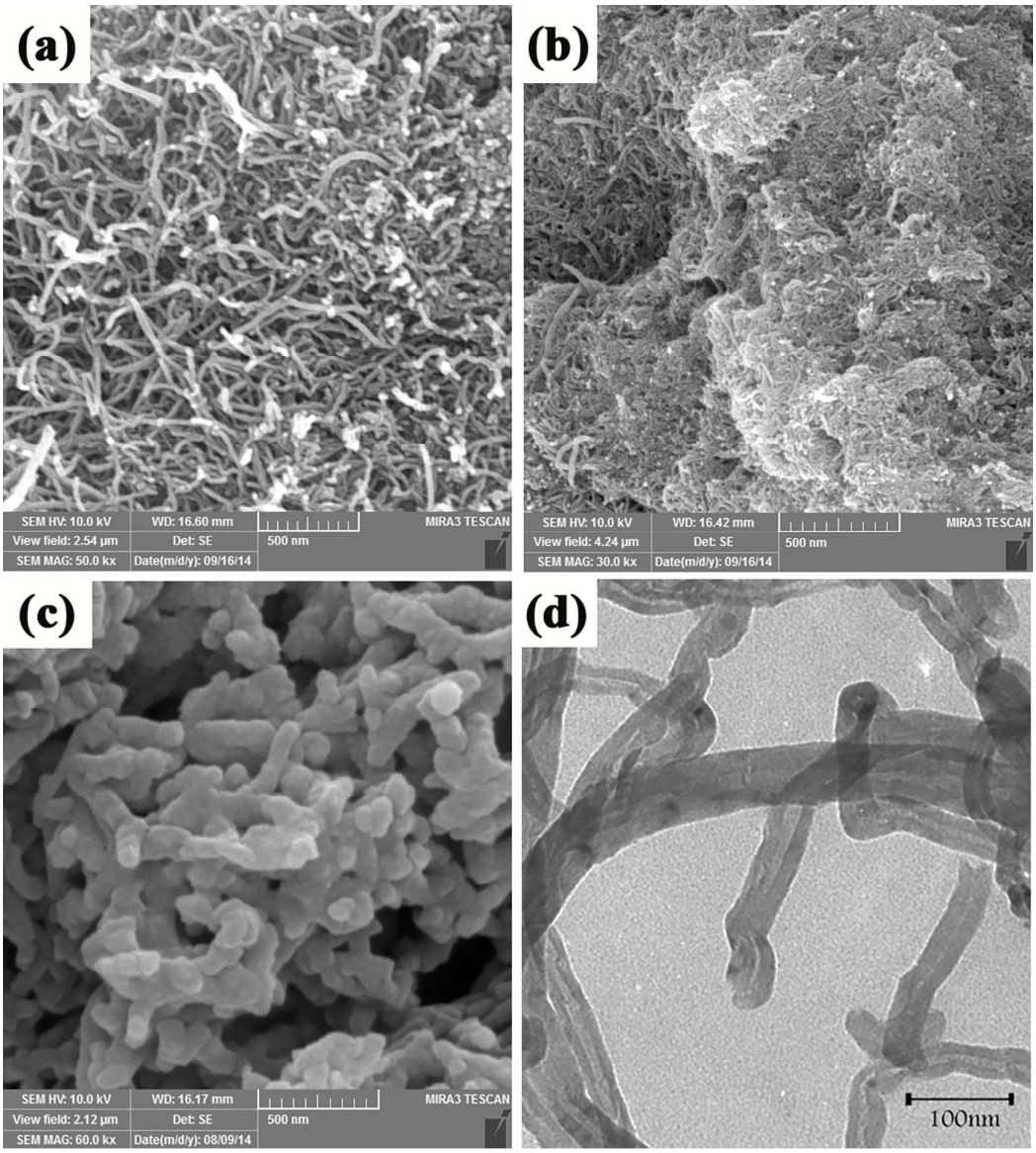

Figure 5. The FE-SEM images of the pure MWCNTs (a), MWCNTs-PEG (b), and MWCNTs-PEG-PANI (c), and TEM image of the MWCNTs-PEG-PANI (d).

Table 1. The electrical properties of the synthesized samples.

Sample	Volume specific resistivity (ρ, Ω.cm)	Electrical conductivity (σ, S cm^{-1})
MWCNTs	0.23	4.34
MWCNTs-COOH	0.46	2.18
MWCNTs-PEG	4.76	0.21
MWCNTs-PEG-PANI[a]	1.19	0.84
PANI[a]	0.84	1.19

[a] The electrical conductivity measurements were achieved at *p*-toluene sulfonic acid-doped state.

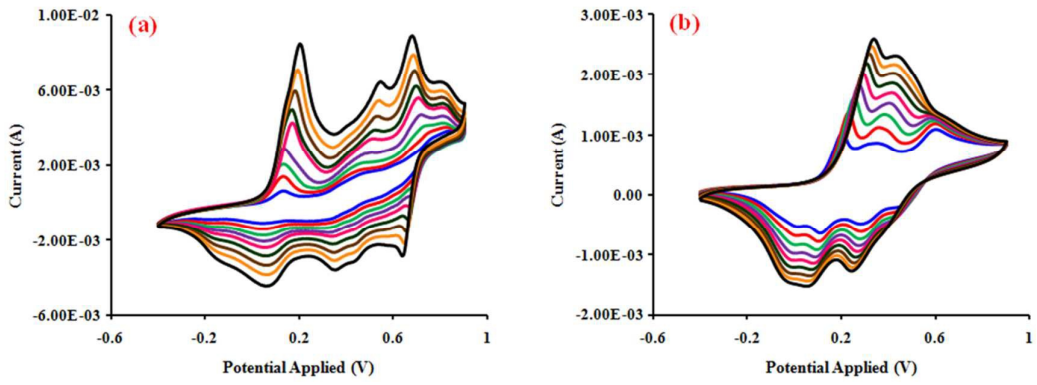

Figure 6. Cyclic voltammetry (CVs) curves of the pure polyaniline (a), and MWCNTs-PEG-PANI nano-hybrid (b).

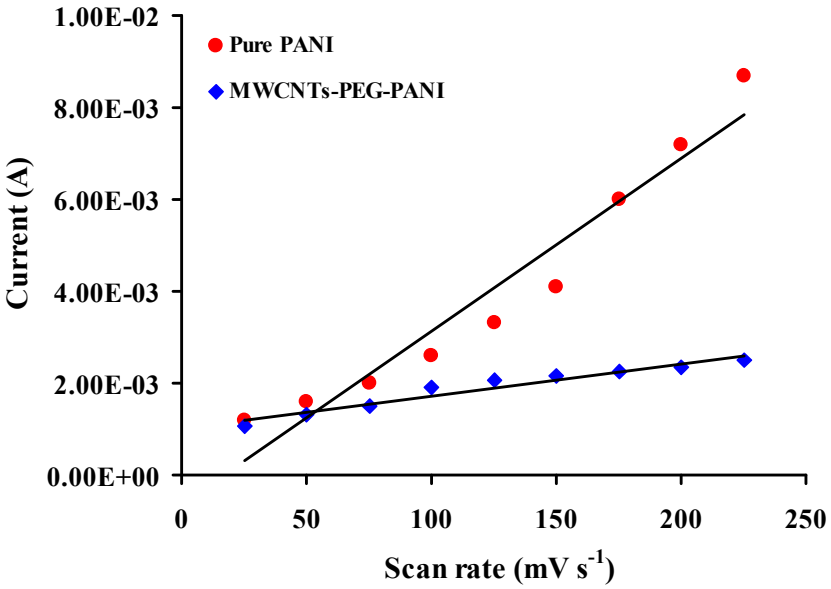

Figure 7. Linear relationship between current and scan rate in the pure polyaniline, and MWCNTs-PEG-PANI (the currents are related to the first anodic peaks).

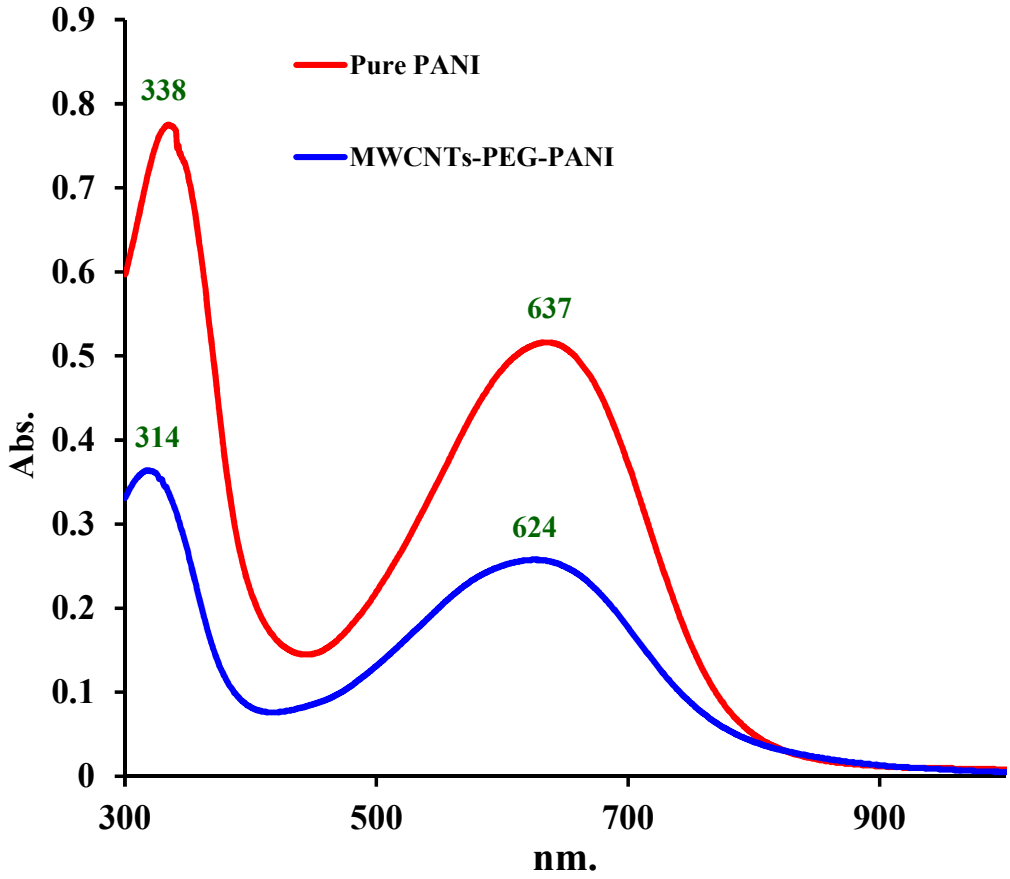

Figure 8. Electronic spectra of the pure PANI, and MWCNTs-PEG-PANI in *N*-methylpyrrolidone (NMP) solution.